Cell-penetrating Helical Peptides Having L-Arginines and Five-membered Ring α,α-Disubstituted α-Amino Acids

Takuma Kato, Makoto Oba, Koyo Nishida, Masakazu Tanaka*

Graduate School of Biomedical Sciences, Nagasaki University, 1-14 Bunkyo-machi, Nagasaki 852-8521, Japan

*Corresponding author

moba@nagasaki-u.ac.jp

ABSTRACT

Cell-penetrating peptides are powerful tools in the delivery of drugs, proteins, and nucleic acids into cells; therefore, a focus has recently been placed on their development. In this study, we synthesized seven types of peptides possessing three L-arginines (L-Arg) and six L-leucines (L-Leu) and/or 1-aminocyclopentane-1-carboxylic acids (Ac_5c), and investigated their secondary structures and cell-penetrating abilities. The peptide composed of an equal number of L-Arg, L-Leu, and Ac_5c formed $3_{10}/\alpha$-helical structures in TFE solution and exhibited the highest cell-penetrating ability of all the peptides examined. Additional cellular uptake studies revealed that the incorporation of Ac_5c into peptides led to improved tolerability against serum. The results of the present study will help in the design of novel cell-penetrating peptides.

INTRODUCTION

Many studies have focused on developing delivery systems for drugs, proteins, nucleic acids, and nano-sized materials, the internalization of which is difficulty in cultured cells and animal tissues.[1-4] A peptide-based system using a cell-penetrating peptide represents a promising delivery system. Several types of cell-penetrating systems have recently been developed for amphiphilic peptides and arginine (Arg)-rich peptides.[5-11] A cationic guanidino group in the side chain of Arg was shown to play a crucial role in the cell-penetrating abilities of Arg-rich peptides. Therefore, a concerted effort has been made to develop novel cell-penetrating peptides based on Arg-rich peptides including their derivatives, which possess guanidino functional groups.[9-14] Furthermore, the structures of the amino acids and amino acid sequences in these peptides may be responsible for the marked differences reported in their cell permeabilities, and this may be due to the different secondary structures of the peptides.[15,16] Appropriate positions of guanidino functional groups in the stable helical structures contributed to better cell permeability. Thus, the design of new cell-penetrating peptides is important to control these secondary structures.

α-Methylated or cyclic α,α-disubstituted α-amino acids (dAAs) have been shown to induce the formation of a stable peptide with a helical secondary structure by being incorporated into oligopeptides composed of protein α-amino acids.[17-20] The number of the dAAs introduced into the peptides and the length of the peptide sequence often affect the types of helical structures, either α-helix or 3_{10}-helix.[21-24] Therefore, dAAs have been used as helix inducers to direct functional peptides such as catalysts and inhibitors.[25-30] dAAs are the powerful tools that are used to design peptide foldamers

In the present study, we designed cell-penetrating helical peptides, which were equipped with the properties of Arg-rich peptides and dAA-containing peptides. The cell-penetrating peptides

described herein were nonapeptides possessing three L-Arg and six L-leucines (L-Leu) and/or 1-aminocyclopentane-1-carboxylic acids (Ac_5c)[31,32] (Figures 1a and 1b). L-Leu and Ac_5c had similar structures with the same number of carbon atoms in the side chain. Nonapeptides were known to represent the borderline region between α-helical and 3_{10}-helical structures. We speculated that the incorporation of the five-membered ring amino acid Ac_5c into the peptides may stabilize the helical secondary structures, and its number in the peptide sequences may also affect the types of helical structures. Figure 1c showed the α-helical and 3_{10}-helical structures formed by the nonapeptides designed in the present study. One α-helical turn consisted of 3.6 amino acid residues and one 3_{10}-helical turn consisted of 3.0 amino acid residues. Therefore, L-Arg appeared at the half side of the α-helical structure, while L-Arg was located in the corner of the triangle of 3_{10}-helical structure (Figure 1c). The nonapeptides formed different secondary structures based on the number of Ac_5c incorporated. An evaluation of cell-penetrating abilities indicated that peptides with three Ac_5c and three L-Leu exhibited the highest cell-permeability. These results will be beneficial for the future design and preparation of novel cell-penetrating peptides

RESULTS

Peptide Synthesis. All peptides were synthesized using Fmoc solid-phase methods. Briefly, Fmoc-L-Arg(Pbf), Fmoc-L-Leu, Fmoc-Gly, and Fmoc-Ac_5c were used as amino acids, and HBTU/HOBt or HATU/HOAt were used as coupling reagents. The coupling of Fmoc-L-Arg(Pbf), Fmoc-L-Leu, and Fmoc-Gly was performed using HBTU/HOBt. On the other hand, hindered Fmoc-Ac_5c and 5(6)-carboxyfluorescein (5(6)-CF) were introduced into the peptides by HATU/HOAt with double coupling. The peptides synthesized were then purified with reversed-phase HPLC (RP-

HPLC). The homogeneity of the purified peptides was verified by analytical RP-HPLC and matrix-assisted laser desorption-ionization time-of-flight mass spectrometry (MALDI-TOF-MS) (Supporting Information). Analytical RP-HPLC of peptides **3b** and **6b** revealed a shoulder peak next to a major peak, which may have been due to the 5- and 6-isomers of CF (Supporting Information).

Secondary Structures of peptides. The CD spectra of nonapeptides **1a**-**7a** were measured in 2,2,2-trifluoroethanol (TFE) solution to obtain information on their secondary structures (Figure 2a). Negative maxima at 205–209 nm ($\pi\rightarrow\pi^*$) and 222–225 nm ($n\rightarrow\pi^*$) were diagnostic of right-handed (*P*) helical structures.[33-36] The ratio of *R* ($\theta_{n\rightarrow\pi^*}/\theta_{\pi\rightarrow\pi^*}$) has been used as a parameter to distinguish α-helical from 3_{10}-helical structures (i.e., $R \approx 1$: α-helix; $R \leq 0.4$: 3_{10}-helix). The CD spectra, except for those of peptides **6a** and **7a**, showed negative maxima at 204–208 and 221–226 nm, which indicated the existence of right-handed (*P*) helices in TFE solution (Figure 2a).[37,38] The intensities of negative maxima decreased with increase in the number of Ac_5c incorporated, which might be due to the difference of the achiral Ac_5c and chiral L-Leu residues. Achiral Ac_5c could not control helical screw-sense of peptides, leading to a decrease of intensities in CD spectra. The ratio of *R* ($\theta_{n\rightarrow\pi^*}/\theta_{\pi\rightarrow\pi^*}$) suggested that the dominant secondary structure of peptides **1a** ($R = 0.52$) and **2a** ($R = 0.52$) was a 3_{10}-helix, while that of peptides **3a** ($R = 0.71$) and **4a** ($R = 0.68$) was a mixture of 3_{10}- and α-helices and that of peptide **5a** ($R = 0.96$) was an α-helix. The CD spectra of peptides **6a** and **7a** did not have characteristic maxima for helical structures. Further CD spectra measurements of peptides **1a** and **4a** were performed in CH_3CN, 90% CH_3CN/H_2O, 50% CH_3CN/H_2O, 10% CH_3CN/H_2O, and H_2O solution (Figures 2b and 2c). In CH_3CN solution, peptide **1a** formed a 3_{10}-helical structure ($R = 0.29$) and peptide **4a** formed 3_{10}/α-helices ($R = 0.68$). Peptide **1a** markedly

changed its secondary structure from a 3_{10}-helix to a random coil with increase in the ratio of H_2O (Figure 2b). On the other hand, peptide **4a** appeared to form a (*P*) helical structure, even in 50% CH_3CN/H_2O solution (Figure 2c). However, the intensities of negative maxima at 205–209 nm ($\pi\rightarrow\pi^*$) and 222–225 nm ($n\rightarrow\pi^*$) were too low to form ideal helices, which implied that the helical secondary structures and/or helical screw-sense of peptide **4a** were not completely controlled.

Cellular Uptake. The cellular uptake of peptides **1b**-**7b** into HeLa cells was evaluated at different concentrations (Figure 3a) and incubation times (Figure 3b). Figure 3a revealed that the uptake of peptides was slightly enhanced by an increase in the number of Ac_5c, reached a maximum at peptide **4b**, which possessed three Ac_5c, and then decreased to peptide **7b**. The cellular uptake of peptide **4b** was significantly higher than that of the others, especially at low concentrations of 25, 50, and 100 nM ($P < 0.01$). The cellular uptake of peptide **4b** was also more efficient than that of the others at all incubation times (Figure 3b). An incubation period of approximately 2 h was optimal for all the peptides examined. The decrease observed in cellular uptake at longer incubation times appeared to be influenced strongly by the lower number of Ac_5c in peptides. The cellular uptake of peptides **1b** and **2b** with 24- and 36-h incubation periods was markedly lower than that with the 2-h incubation, while that of peptides **6b** and **7b** was not.

The cellular uptake of peptides **1b**, **4b**, and **6b** after the pre-incubation of each peptide with medium containing serum was evaluated in order to determine why the cellular uptake of peptide **4b** was the highest (Figure 4a). Peptides and proteins are easily degraded by proteases in the serum; therefore, the tolerability of peptides to proteases could be investigated in this experiment. The cellular uptake of peptide **1b**, which had no Ac_5c, was markedly lower than that of peptide **4b** and **6b** following an increase in the pre-incubation. The cellular uptake of peptide **6b** remained unchanged even after a

2-h pre-incubation (**6b** vs **1b** and **4b**, $P < 0.01$). These results indicated that the incorporation of Ac5c into peptides enhanced their stability in medium containing serum.

An additional cellular uptake experiment was performed with post-incubation after the replacement of peptide-containing medium with fresh medium in order to gain further insights into peptides **1b**, **4b**, and **6b** (Figure 4b). All peptides showed similar results in that 50% of all the peptides examined were eliminated from the HeLa cells after the 4-h post-incubation, which implied that all peptides had the same fate after their cellular uptake.

Confocal Laser Scanning Microscopy (CLSM) Observations. Drug delivery vehicles sometimes possess different cellular uptake mechanisms and intracellular destinations depending on the structures of vehicles.[39-42] The intracellular distribution of peptides **1b**, **4b**, and **6b** (green) was investigated using CLSM (Figure 5). LysoTracker Red (red) and Hoechst33342 (blue) were used to label late endosomes/lysosomes and nuclei, respectively. The intensity of the observed green signals was the highest in HeLa cells treated with peptide **4b** (Figures 5a-c), which was consistent with the cellular uptake results shown in Figure 3. The intracellular distribution of all three peptides was mainly observed as yellow spots and also as green spots. Furthermore, internalization of each peptide into the HeLa cells was confirmed by CLSM observations with treatment of trypan blue (Figure S5), which was consistent with the results in Figure 5. Trypan blue was known not to permeate the cell membrane and to quench extracellular fluorescent probes.[43,44] The colocalization of the peptides with late endosomes/lysosomes was quantified and is shown in Figure 5d. All peptides showed similar colocalization ratios at approximately 40% and were not significantly different. The distribution of peptides was not observed in the nuclei of HeLa cells treated with all three peptides. These results indicated that the peptides described here appeared to be internalized

into HeLa cells via the same mechanism regardless of the number of Ac_5c or the secondary structures of the peptides.

DISCUSSION

In the present study, two distinctive functions, that of Arg-rich peptides and also that of dAA-containing peptides, were integrated into the design of cell-penetrating peptides. The five-membered ring dAA, Ac_5c, was used to modulate the secondary structures of peptides. CD spectra revealed that the dominant structures of nonapeptide **1a**-**7a** in TFE solution differed according to the number of Ac_5c introduced (Figure 2a). Peptide **1a**, which had no Ac_5c, formed a 3_{10}-helical structure, while peptide **5a**, which had four Ac_5c, formed an α-helical structure. Increasing the number of Ac_5c enhanced the α-helicity of the peptides examined. Nonapeptides **6a** and **7a** in TFE solution showed no characteristic maxima for helical structures. Two explanations have been proposed. The first is that there were more achiral amino acids in nonapeptides **6a** and **7a** than in the other peptides, leading to an inability to control the helical screw-sense. Equal amounts of right-handed (*P*) and left-handed (*M*) helices should show almost no maxima in the CD spectrum. The second is the formation of aggregates. Aggregation was sometimes detected with high concentrations of peptide **7a**. The CD spectrum measurement of nonapeptide **7a** may not have been conducted correctly. Additional CD spectra measurements of peptides **1a** and **4a** in CH_3CN/H_2O solution revealed the stability of their helical secondary structures against H_2O. Peptide **1a** could not form helical structures, even in 90% CH_3CN/H_2O solution, while peptide **4a** partially maintained helical structures, even in 50% CH_3CN/H_2O solution. Furthermore, peptide **2a** showed similar results of peptide **1a** and peptide **3a** could not form helical structures in 50% CH_3CN/H_2O solution

(Figure S3). These results demonstrated that the incorporation of Ac_5c in peptides stabilized their helical structures, even in aqueous solution.

Cellular uptake experiments indicated that peptide **4b**, which had three Ac_5c, exhibited the highest cell permeability of all the peptides examined (Figure 3). It is worth mentioning that the cellular uptaken amount of peptide **4b** was significantly higher than that of HIV-TAT peptide (Figure S4), which was one of the most famous Arg-rich cell-penetrating peptides.[45] The dominant structure of nonapeptide **4a** was $3_{10}/\alpha$-helices in TFE solution (Figure 2a). The helicity of peptide **4a** was partly maintained in 50% H_2O solution, while that of peptide **1a**-**3a** was not (Figures 2b, 2c, and S3). As shown in Figure 1c, if the peptides described in the present study formed a 3_{10}-helical structure, L-Arg was located in one corner of the triangle. Previous study examining amphiphilic α-helical cell-penetrating peptides reported that it was important for the function of these peptides to concentrate hydrophobic amino acids and cationic amino acids in one direction.[15,16,46] The 3_{10}-helical structure is more appropriate for the peptides designed here than the other structures, including the α-helical structure, due to the concentration of L-Arg in one region. This appeared to be one reason why peptide **4**, which formed $3_{10}/\alpha$-helices in TFE solution and maintained its helicity even in 50% H_2O solution, exhibited the highest cell permeability. The pre-incubation of peptides in medium containing serum affected their cell permeability in a manner that depended on the number of Ac_5c and pre-incubation times. These results indicated that peptides with Ac_5c may have acquired tolerability to the proteases in the serum (Figure 4a). Ac_5c was a non-proteinogenic amino acid and thus the proteases may have hydrolyzed the peptides containing Ac_5c slowly. The incorporation of dAAs into peptides was previously reported to result in protease resistance, more so than in peptides composed of natural α-amino acids only,[47-50] which is consistent with our results. Cellular uptake experiments with post-incubation after the replacement of peptide-containing medium with fresh

medium did not significantly affect the peptides **1b**, **4b**, and **6b** (Figure 4b). CLSM observations, in which the colocalization of the peptides examined with late endosomes/lysosomes was evaluated, revealed that all three peptides: **1b**, **4b**, and **6b**, were distributed to similar regions following their cellular uptake (Figure 5). Taken together with these results (Figures 4b and 5), the peptides examined in the present study were internalized into the HeLa cells by the same routes and had the same fate. Peptide **4b** was internalized into HeLa cells better than the other peptides, and this was attributed to synergistic effects between the 3_{10}-helical secondary structure and tolerability to proteases. However, the formation of a complete right-handed (*P*) 3_{10}-helical structure was not achieved in the present study. The introduction of achiral Ac_5c into the peptides led to change in the preferred secondary structures from 3_{10}-helix to α-helix and decrease in the right-handed helicity. Further mechanistic investigations of 3_{10}-helical cell-penetrating peptides are warranted to develop more effective cell-penetrating peptides using strictly-controlled 3_{10}-helical peptides.

CONCLUSIONS

We designed and synthesized seven types of nonapeptides possessing three L-Arg and six L-Leu and/or Ac_5c for the cell-penetrating peptides. The number of Ac_5c introduced had an effect on the secondary structures of the peptides. Peptide **4**, which had three Ac_5c, preferred 3_{10}/α-helices and showed the strongest cell-penetrating ability. These results are the successful demonstrations of cell-penetrating peptides equipped with two distinctive functions of Arg-rich peptides and dAA-containing peptides.

EXPERIMENTAL PROCEDURES

General. All commercial materials were used without further purification. Fmoc-L-Leu and piperidine were purchased from Tokyo Chemical Industry Co., Ltd. (Tokyo, Japan). Fmoc-Ac5c was obtained from Watanabe Chemical Industries Co., Ltd. (Hiroshima, Japan). Fmoc-L-Arg(Pbf), Fmoc-Gly, and CLEAR-Amide resin were purchased from the Peptide Institute., Inc. (Osaka, Japan). HBTU, HOBt, HATU, and HOAt were the products of AAPPTec (Louisville, KY). Triisopropylsilane (TIS), 5(6)-CF, acetonitrile, and Dulbecco's modified Eagle's medium (DMEM) were obtained from Sigma-Aldrich Co. (St. Louis, MO). *N*,*N*-Dimethylformamide (DMF), Cell lysis buffer M, and TFE were purchased from Wako Pure Chem. Co., Inc. (Osaka, Japan). Diethyl ether was the product from Kanto Chemical Co., Inc. (Tokyo, Japan). Trifluoroacetic acid (TFA) was obtained from Nacalai Tesque, Co., Inc. (Kyoto, Japan). Hoechst33342 was purchased from Dojindo Laboratories (Kumamoto, Japan). LysoTracker Red was obtained from Molecular Probes (Eugene, OR). The micro bicinchoninic acid (BCA) protein assay reagent kit was from Thermo Fisher Scientific, Inc. (Rockford, IL).

Synthesis and Characterization of Peptides. The peptides were synthesized on solid support by Fmoc solid-phase methods using standard commercially available Rink amide resin and Fmoc-amino acids. The following describes a representative coupling and deprotection cycle at 76-100 μmol scales. First, 200-263 mg of CLEAR-Amide resin (loading: 0.38 mmol/g) was soaked overnight in DMF. After DMF had been removed, 20% piperidine in DMF was added to the resin for deprotection. After removing and washing out piperidine, Fmoc-amino acid (3 equiv) and HBTU/HOBt or HATU/HOAt (3 equiv) dissolved in DMF (1.4 mL) were added for the coupling reaction (coupling reagents: HBTU/HOBt for Fmoc-L-Leu, Fmoc-L-Arg(Pbf), and Fmoc-Gly; HATU/HOAt for Fmoc-Ac5c and 5(6)-CF with double coupling). The resin was then suspended in

cleavage cocktail (TFA: 1.9 mL; H_2O: 50 μL; TIS: 50 μL). The TFA solution was evaporated to a small volume and added to cold diethyl ether to precipitate the peptides. The dried crude peptides were dissolved in acetonitrile and/or H_2O, and then purified by RP-HPLC using a COSMOSIL Packed Column 5C_{18}-AR-II (20 ID x 250 mm) (Nacalai). Freeze-drying afforded colorless or yellow crystals, which were characterized by analytical RP-HPLC (COSMOSIL Packed Column 5C_{18}-AR-II, 4.6 ID x 250 mm) and MALDI-TOF-MS (Bruker Daltonics Ultraflex, Fremont, CA). RP-HPLC was performed utilizing JASCO-PU-2089 Plus (JASCO, Tokyo, Japan) with a JASCO-2075-Plus as a detector, with being both controlled by JASCO BORWIN software. Solvent A: 0.05% TFA in H_2O; solvent B: 0.05% TFA in acetonitrile. The purification procedure required gradient conditions (from 95% to 50% solvent A over 20 min) with a flow rate of 10 mL/min and detection at 220 nm. The purity of the final compounds was further confirmed using similar RP-HPLC conditions (from 95% to 35% solvent A over 20 min, then from 35% to 10% solvent A over 5 min); however, the flow rate was changed for 1 mL/min.

CD Spectrum Measurement. CD spectra were recorded with a JASCO J-725N spectropolarimeter (JASCO) using a 1.0 mm path length cell. Data are expressed in terms of $[\Theta]_R$, in other words, residue molar ellipticity ($deg \cdot cm^2 \cdot dmol^{-1}$). TFE, CH_3CN, and H_2O were used as solvents.

Cellular Uptake. HeLa cells were seeded onto 96-well culture plates (10000 cells/well) and incubated in 100 μL of DMEM containing 10% fetal bovine serum (FBS). The medium was then replaced with fresh medium containing 10% FBS, and a peptide solution was added to each well at an appropriate concentration (Figure 3) and at 100 nM (Figure 4b). In the case of Figure 4a, the medium was replaced with pre-incubated medium (containing 10% FBS), which had been incubated

with 100 nM of each peptide at 37˚C for 0.5, 1, or 2 h. After each time incubation (Figure 3) and a 2-h incubation (Figure 4a), the medium was removed, and the cells were washed 3 times with ice-cold PBS supplemented with heparin (20 units/mL) and then treated with Cell lysis buffer M. In the case of Figure 4a, after a 2-h incubation, the peptide-containing medium was replaced with fresh medium. After each post-incubation time, the medium was removed, and the cells were washed 3 times with ice-cold PBS supplemented with heparin (20 units/mL) and then treated with Cell lysis buffer M. The fluorescence intensity of each lysate was measured using a spectrofluorometer (ND-3300, NanoDrop, Wilmington, DE). The amount of protein in each well was concomitantly determined using the BCA protein assay reagent kit. The results are presented as the mean and standard deviation obtained from 6 samples (Figures 3a and 4) or 3 samples (Figure 3b).

CLSM observations. HeLa cells were seeded onto 8-well chambered cover glasses (Iwaki, Tokyo, Japan) (20000 cells/well) and incubated overnight in 200 μL of DMEM containing 10% FBS. The medium was then replaced with fresh medium containing 10% FBS, and a peptide solution was applied to each well at a concentration of 1 μM. After a 2-h incubation, the medium was removed, and the cells were washed 3 times with ice-cold PBS supplemented with heparin (20 units/mL). The intracellular distribution was observed by CLSM after staining late endosomes/lysosomes with LysoTracker Red and nuclei with Hoechst33342. CLSM observations were performed using LSM 710 (Carl Zeiss, Oberlochen, Germany) with a Plan-Apochromat 63x/1.4 objective (Carl Zeiss) at an excitation wavelength 405 nm (UV laser) for Hoechst33342, 488 nm (Ar laser) for peptides, and 543 nm (He-Ne laser) for LysoTracker Red. The rate of the colocalization of peptides with LysoTracker Red was quantified.[51] The colocalization ratio was quantified as follows:

$$\text{Colocalization ratio (\%)} = \text{peptide pixels}_{\text{colocalization}} / \text{peptide pixels}_{\text{total}} \times 100$$

where peptide $pixels_{colocalization}$ represents the number of peptide pixels colocalizing with LysoTracker Red in the cell, and peptide $pixels_{total}$ represents the number of all the pixels in the cell. The results are represented as the mean and standard deviation obtained from 15 cells.

Statistical Analysis. Significance was assessed by a 2-tailed Student's *t*-test. *P* values of less than 0.05 were considered significant.

ASSOCIATED CONTENT

Supporting Information

MALDI-TOF-MS data and copies of analytical RP-HPLC of peptides **1a**-**7a** and **1b**-**7b**. This material is available free of charge via the Internet at http://pubs.acs.org.

AUTHOR INFORMATION

Corresponding Author

*E-mail: moba@nagasaki-u.ac.jp ; Tel (+81)95-819-2424; Fax: (+81)95-819-2424.

Notes

The authors declared no competing financial interest.

ACKNOWLEDGEMENTS

This work was financially supported in part by JSPS KAKENHI Grant Number 25713008 and by a Grant from the Takeda Science Foundation.

ABBREVIATIONS

Ac$_5$c, 1-aminocyclopentane-1-carboxylic acid; BCA, bicinchoninic acid; CD, circular dichroism; CF, carboxyfluorescein; CLSM, confocal laser scanning microscope; dAA, α,α-disubstituted α-amino acid; DMEM, Dulbecco's modified Eagle's medium; DMF, *N*,*N*-dimethylformamide; FBS, fetal bovine serum; Fmoc, 9-fluorenylmethoxycarbonyl; HATU, *O*-(7-azabenzotriazol-1-yl)-1,1,3,3-tetramethyluronium hexafluorophosphate; HBTU, *O*-benzotriazol-1-yl-*N*,*N*,*N'*,*N'*-tetramethyluronium hexafluoro-phosphate; HOAt, 1-hydroxy-7-azabenzotriazole; HOBt, 1-hydroxybenzotriazole; MALDI-TOF-MS, matrix-assisted laser desorption-ionization time-of-flight mass spectrometry; Pbf, 2,2,4,6,7-pentamethyldihyrdobenzofuran-5-sulfonyl; RP, reversed-phase; TFA; trifluoroacetic acid; TFE, 2,2,2-trifluoroethanol; TIS, triisopropylsilane.

REFERENCES

1. Wagner, E., Curiel, D., Cotton, M. (1994) Delivery of drugs, proteins and genes into cells using transferrin as a ligand for receptor-mediated endocytosis. *Adv. Drug Deliv. Rev. 14*, 113–135.
2. Uekama, K., Hirayama, F., Irie, T. (1998) Cyclodextrin drug carrier systems. *Chem. Rev. 98*, 2045–2076.
3. Mintzer, M. A., Simanek, E. E. (2009) Nonviral vectors for gene delivery. *Chem. Rev. 109*, 259–302.

4. Oba, M. (2013) Study on development of polymeric micellar gene carrier and evaluation of its functionality. *Biol. Pharm. Bull. 36*, 1045–1051.
5. Nakase, I., Takeuchi, T., Tanaka, G., Futaki, S. (2008) Methodological and cellular aspects that govern the internalization mechanisms of arginine-rich cell-penetrating peptides. *Adv. Drug Deliv. Rev. 60*, 598–607.
6. Schmidt, N., Mishra, A., Lai, G. H., Wong, G. C. L. (2010) Arginine-rich cell-penetrating peptides. *FEBS Lett. 584*, 1806–1813.
7. EI-Sayed, A., Futaki, S., Harashima, H. (2009) Delivery of macromolecules using arginine-rich cell-penetrating peptides: ways to overcome endosomal entrapment. *AAPS J. 11*, 13–22.
8. Copolovici, D. M., Langel, K., Eriste, E., Langel, U. (2014) Cell-penetrating peptides: design, synthesis, and applications. *ACS Nano 8*, 1972–1994.
9. Umezawa, N., Gelman, M. A., Haigis, M. C., Raines, R. T., Gellman, S. H. (2001) Translocation of a β-peptide across cell membranes. *J. Am. Chem. Soc. 124*, 368–369.
10. Potocky, T. B., Menon, A. K., Gellman, S. H. (2003) Cytoplasmic and nuclear delivery of a TAT-derived peptide and β-peptide after endocytic uptake into HeLa cells. *J. Biol. Chem. 278*, 50188–50194.
11. Nakase. I., Akita, H., Kogure, K., Graslund, A., Langel, U., Harashima, H., Futaki, S. (2012) Efficient intracellular delivery of nucleic acid pharmaceuticals using cell-penetrating peptides. *Acc. Chem. Res. 45*, 1132–1139.
12. Liu, C., Liu, X., Rocchi, P., Qu, F., Iovanna, J. L., Peng, L. (2014) Arginine-terminated generation 4 PAMAM dendrimer as an effective nanovector for functional siRNA delivery in vitro and in vivo. *Bioconjugate Chem. 25*, 521–532.

13. Maiti, K. K., Lee, W. S., Takeuchi, T., Watkins, C., Fretz, M., Kim, D.-C., Futaki, S., Jones, A., Kim, K.-T., Chung, S.-K. (2007) Guanidine-containing molecular transporters: sorbitol-based transporters show high intracellular selectivity toward mitochondria. *Angew. Chem. Int. Ed. 46*, 5880–5884.

14. Fillon, Y. A., Anderson, J. P., Chmielewski, J. (2005) Cell penetrating agents based on a polyproline helix scaffold. *J. Am. Chem. Soc. 127*, 11798–11803.

15. Potocky, T. B., Menon, A. K., Gellman, S. H. (2005) Effects of conformational stability and geometry of guanidinium display on cell entry by β-peptides. *J. Am. Chem. Soc. 127*, 3686–3687.

16. Yamashita, H., Demizu, Y., Shoda, T., Sato, Y., Oba, M., Tanaka, M., Kurihara, M. (2014) Amphipathic short helix-stabilized peptides with cell-membrane penetrating ability. *Bioorg. Med. Chem. 22*, 2403–2408.

17. M. Tanaka (2007) Design and synthesis of chiral α,α-disubstituted amino acids and conformational study of their oligopeptides. *Chem. Pharm. Bull. 55*, 349–358.

18. Venkatraman, J., Shankaramma, S. C., Balaram, P. (2001) Design of folded peptides. *Chem. Rev. 101*, 3131–3152.

19. Karle, I. L. (2001) Controls exerted by the Aib residue: helix formation and helix reversal. *Biopolymers (Peptide Science) 60*, 351–365.

20. Karle, I. L. (1999) Aspects of peptide folding and aggregation. *Acc. Chem. Res. 32*, 693–701.

21. Toniolo, C., Crisma, M., Formaggio, F., Peggion, C. (2001) Control of peptide conformation by the Thorpe-ingold effect (Cα-tetrasubstitution). *Biopolymers (Peptide Science) 60*, 396–419.

22. Karle, I. L., Balaram, P. (1990) Structural characteristics of α-helical peptide molecules containing Aib residues. *Biochemistry 29*, 6747–6756.

23. Demizu, Y., Doi, M., Kurihara, M., Okuda, H., Nagano, M., Suemune, H., Tanaka, M. (2011) Conformational studies on peptides containing α,α-disubstituted α-amino acids: chiral cyclic α,α-disubstituted α-amino acid as an α-helical inducer. *Org. Biomol. Chem. 9*, 3303–3312.

24. Haynes, S. R., Hagius, S. D., Juban, M. M., Elzer, P. H., Hammer, R. P. (2005) Improved solid-phase synthesis α,α-dialkylated amino acid-rich peptides with antimicrobial activity. *J. Pept. Sci. 66*, 333–347.

25. Licini, G., Bonchio, M., Broxterman, Q. B., Kaptein, B., Moretto, A., Toniolo, C., Scrimin, P. (2006) C^{α}-Tetrasubstituted amino acid based peptides in asymmetric catalysis. *Biopolymers (Peptide Science) 84*, 97–104.

26. Sissi, C., Rossi, P., Felluga, F., Formaggio, F., Palumbo, M., Tecilla, P., Toniolo, C., Scrimin, P. (2001) Dinuclear Zn^{2+} complexes of synthetic heptapeptides as artificial nucleases. *J. Am. Chem. Soc. 123*, 3169–3170.

27. Nagano, M., Doi, M., Kurihara, M., Suemune, H., Tanaka, M. (2010) Stabilized α-helix-catalyzed enantioselective epoxidation of α,β-unsaturated ketones. *Org. Lett. 12*, 3564–3566.

28. Yokum, T. S., Elzer, P. H., McLaughlin, M. L. (1996) Antimicrobial α,α-dialkylated amino acid rich peptides with *in-vivo* activity against an intracellular pathogen. *J. Med. Chem. 39*, 3603–3605.

29. Moellering, R. E., Cornejo, M., Davis, T. N., Bianco, C. D., Aster, J. C., Blacklow, S. C., Kung, A. L., Gilliland, D. G., Verdine, G. L., Bradner, J. E. (2009) Direct inhibition of the NOTCH transcription factor complex. *Nature 462*, 182–190.

30. Schafmeister, C. E., Po, J., Verdine, G. L. (2000) An all-hydrocarbon cross-linking system for enhancing the helicity and metabolic stability of peptides. *J. Am. Chem. Soc. 122*, 5891–5892.

31. Bardi, R., Piazzesi, A. M., Toniolo, C., Sukumar, M., Balaram, P. (1986) Stereochemistry of peptides containing 1-aminocyclopentanecarboxylic acid (Acc^5): Solution and solid-state conformations of Boc-Acc^5-Acc^5-NHMe. *Biopolymers 25*, 1635–1644.

32. Santini, A., Barone, V., Bavoso, A., Benedetti, E., Di Blasio, B., Fraternali, F., Lelj, F., Pavone, V., C. Pedone, Crisma, M., Bonora, G. M., Toniolo, C. (1988) Structural versatility of peptides from $C^{\alpha,\alpha}$-dialkylated glycines: a conformation energy calculation and X-ray diffraction study of homopeptides from 1-aminocyclopentane-1-carboxylic acid. *Int. J. Biol. Macromol. 10*, 292–299.

33. Yokum, T. S., Gauthier, T. J., Hammer, R. P., McLaughlin, M. L. (1997) Solvent effects on the 3_{10}-/α-helix equilibrium in short amphipathic peptides rich in α,α-disubstituted amino acids. *J. Am. Chem. Soc. 119*, 1167–1168.

34. Chang, C. T., Wu, C.-S. C., Yang, J. T. (1978) Circular dichroic analysis of protein conformation: inclusion of the β-turns. *Anal. Biochem. 91*, 13–31.

35. Brahms, S., Brahms, J. (1980) Determination of protein secondary structure in solution by vacuum ultraviolet circular dichroism. *J. Mol. Biol. 138*, 149–178.

36. Manning, M. C., Woody, R. W. (1991) Theoretical CD studies of polypeptide helices: Examination of important electronic and geometric factors. *Biopolymers 31*, 569–586.

37. Toniolo, C., Polese, A., Formaggio, F., Crisma, M., Kamphuis, J. (1996) Circular dichroism spectrum of a peptide 3_{10}-helix. *J. Am. Chem. Soc. 118*, 2744–2745.

38. Pengo, P., Pasquato, L., Moro, S., Brigo, A., Fogolari, F., Broxterman, Q. B., Kaptein, B., Scrimin, P. (2003) Quantitative correlation of solvent polarity with the α-/3_{10}-helix equilibrium: a heptapeptide behaves as a solvent-driven molecular spring. *Angew. Chem. Int. Ed. 42*, 3388–3392.

39. von Gersdorff, K., Sanders, N. N., Vandenbroucke, R., De Smedt, S. C., Wagner, E., Ogris, M. (2006) The internalization route resulting in successful gene expression depends on both cell line and polyethyleneimine polyplex type. *Mol. Ther. 14*, 745–753.

40. Khalil, I. A., Kogure, K., Akita, H., Harashima, H. (2006) Uptake pathways and subsequent intracellular trafficking in nonviral gene delivery. *Pharmacol. Rev. 58*, 32–45.

41. Miyata, K., Oba, M., Nakanishi, M., Fukushima, S., Yamasaki, Y., Koyama, H., Nishiyama, N., Kataoka, K. (2008) Polyplexes from poly(aspartamide) bearing 1,2-diaminoethane side chains induce pH-selective, endosomal membrane destabilization with amplified transfection and negligible cytotoxicity. *J. Am. Chem. Soc. 130*, 16287–16294.

42. Uchida, H., Miyata, K., Oba, M., Ishii, T., Suma, T., Itaka, K., Nishiyama, N., Kataoka, K. (2011) Odd-even effect of repeating aminoethylene units in the side chain of N-substituted polyaspartamides on gene transfection profiles. *J. Am. Chem. Soc. 133*, 15524–15532.

43. Thiele, L., Rothen–Rutishauser, B., Jilek, S., Wunderli–Allenspach, H., Merkle, H. P., Walter, E. (2001) Evaluation of particle uptake in human blood monocyte-derived cell in vitro. Does phagocytosis activity of dendric cells measure up with macrophages? *J. Control. Release 76*, 59–71.

44. De Bruin, K., Ruthardt, N., von Gersdorff, K., Bausinger, R., Wagner, E., Ogris, M., Brauchle, C. (2007) Cellular dynamics of EGF receptor-targeted synthetic viruses. *Mol. Ther. 15*, 1297–1305.

45. Frankel, A. D., Pabo, C. O. (1988) Cellular uptake of the Tat protein from human immunodeficiency virus. *Cell 55*, 1189–1193.

46. Geisler, I., Chmielewski, J. (2009) Cationic amphiphilic polyproline helices: side-chain variations and cell-specific internalization. *Chem. Biol. Drug. Des. 73*, 39–45.

47. Wada, S., Tsuda, H., Okada, T., Urata, H. (2011) Cellular uptake of Aib-containing amphipathic helix peptide. *Bioorg. Med. Chem. Lett. 21*, 5688–5691.

48. Zikou, S., Koukkou, A., Mastora, P., Sakarellos-Daitsiotis, M., Sakarellos, C., Drainas, C., Panou-Pomonis, E. (2007) Design and synthesis of cationic Aib-containing antimicrobial peptides: conformational and biological studies. *J. Pept. Sci. 13*, 481–486.

49. Nachman, R. J., Isaac, R. E., Coast, G. M., Holman, G. M. (1997) Aib-containing analogues of the insect kinin neuropeptide family demonstrate resistance to an insect angiotensin-converting enzyme and protein diuretic activity. *Peptides 18*, 53–57.

50. Yamaguchi, H., Kodama, H., Osada, S., Kato, F., Jelokhani–Niaraki, M., Kondo, M. (2003) Effect of α,α-dialkyl amino acids on the protease resistance of peptides. *Biosci. Biotechnol. Biochem. 67*, 2269–2272.

51. Oba, M., Tanaka, M. (2012) Intracellular mechanism of protein transfection reagents. *Biol. Pharm. Bull. 35*, 1064–1068.

Table of Contents

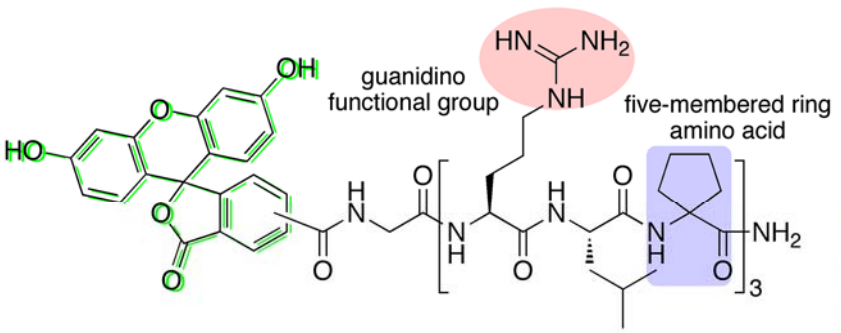

5(6)-CF-Gly-(L-Arg-L-Leu-Ac_5c)$_3$-NH_2

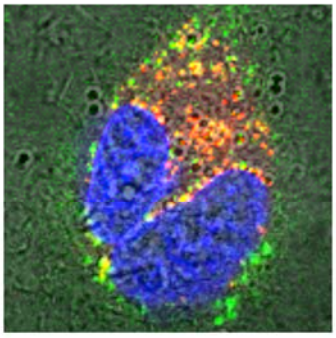

green: peptides blue: nuclei
red: late endosomes/lysosomes

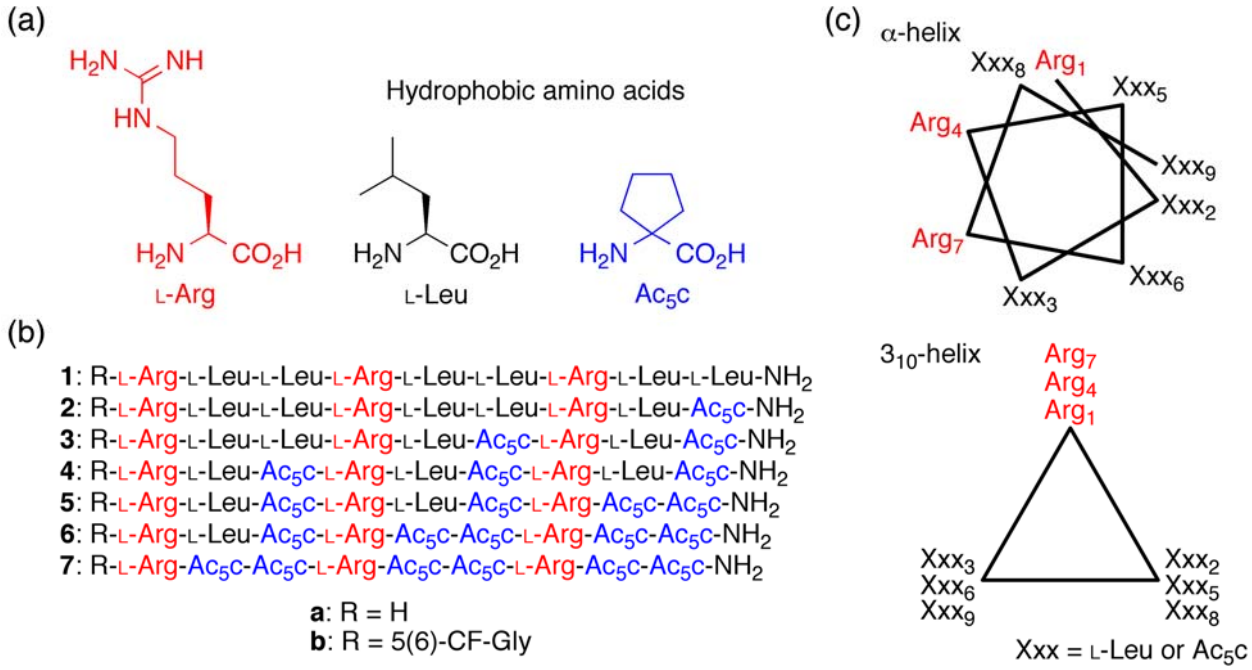

Figure 1. The amino acids, peptides, and helical structures described in the present study. (a) Structures of the amino acids, L-arginine (L-Arg), L-leucine (L-Leu), and 1-aminocyclopentane-1-carboxylic acid (Ac_5c). (b) Sequences of the peptides composed of L-Arg, L-Leu, and Ac_5c with or without a fluorescent label. (c) Schematic illustration of the α-helical and 3_{10}-helical structures as viewed along the helical axis.

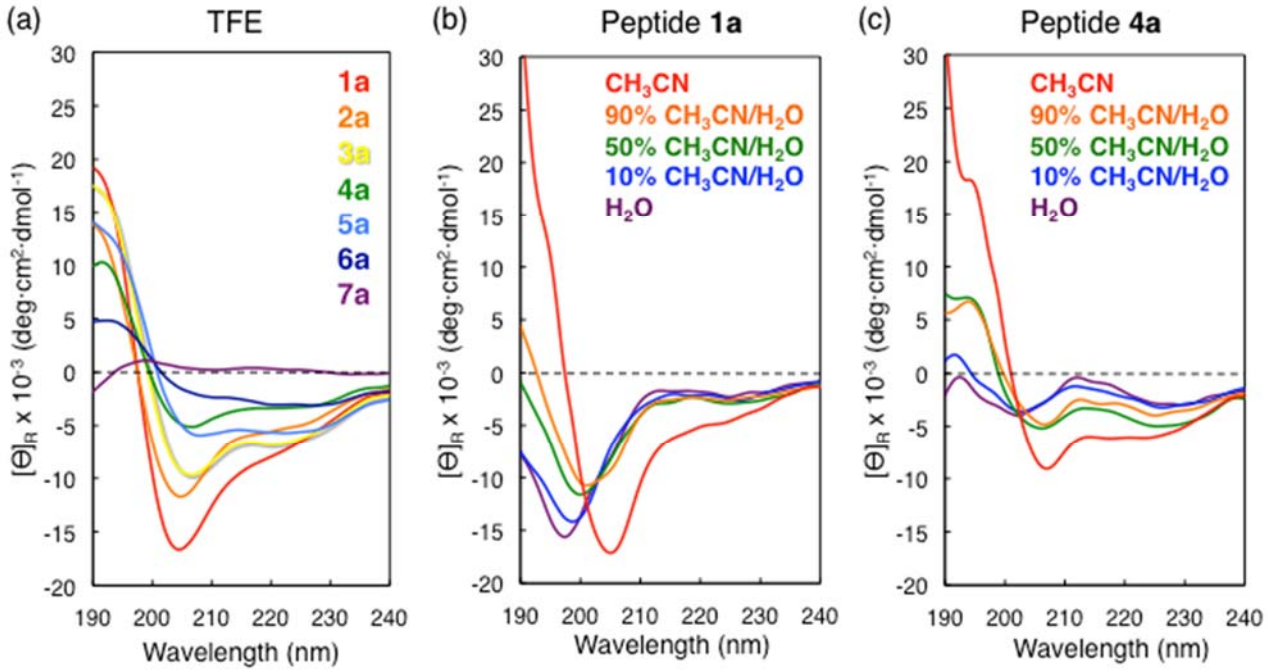

Figure 2. CD spectra of nonapeptides **1a**-**7a** in TFE solution (a). CD spectra of nonapeptides **1a** (b) and **4a** (c) in 100% CH_3CN, 90% CH_3CN/H_2O, 50% CH_3CN/H_2O, 10% CH_3CN/H_2O, and H_2O solution. Peptide concentration: 0.1 mM.

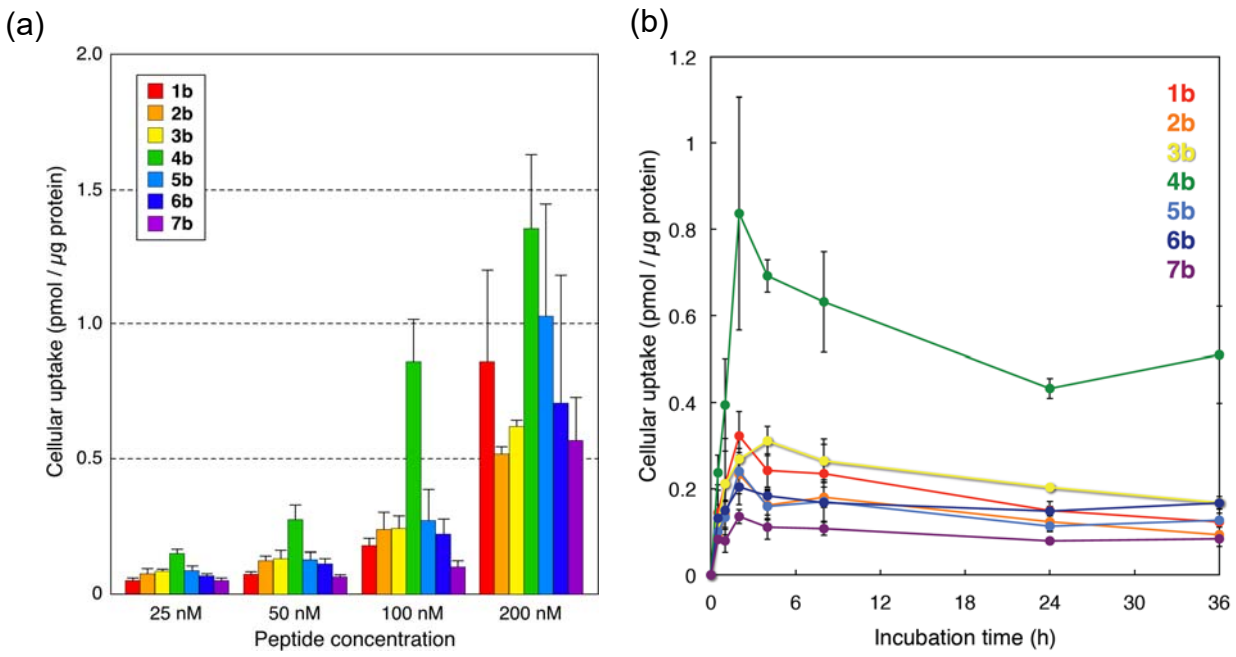

Figure 3. Cellular uptake of peptides **1b**-**7b**. (a) The peptide concentration-dependency with the 2-h incubation period. Error bars represent the standard deviation, n = 6. (b) The incubation time-dependency with a peptide concentration of 100 nM. Error bars represent the standard deviation, n = 3.

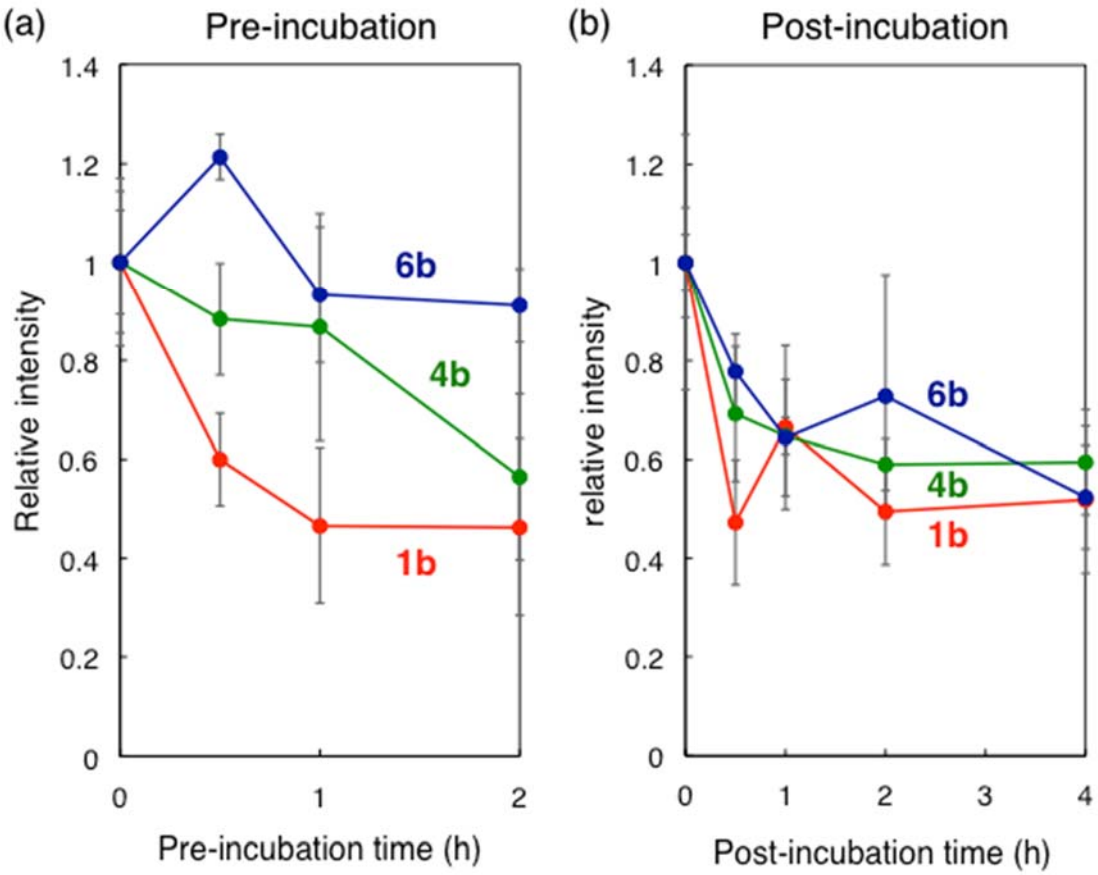

Figure 4. Cellular uptake of peptides **1b**, **4b**, and **6b** under the experimental conditions of (a) each pre-incubation time of peptides in medium containing serum, followed by a 2-h incubation of peptides with cells or (b) a 2-h incubation of peptides with cells, followed by a post-incubation of each time after a replacement with fresh medium. Error bars represent the standard deviation, n = 6.

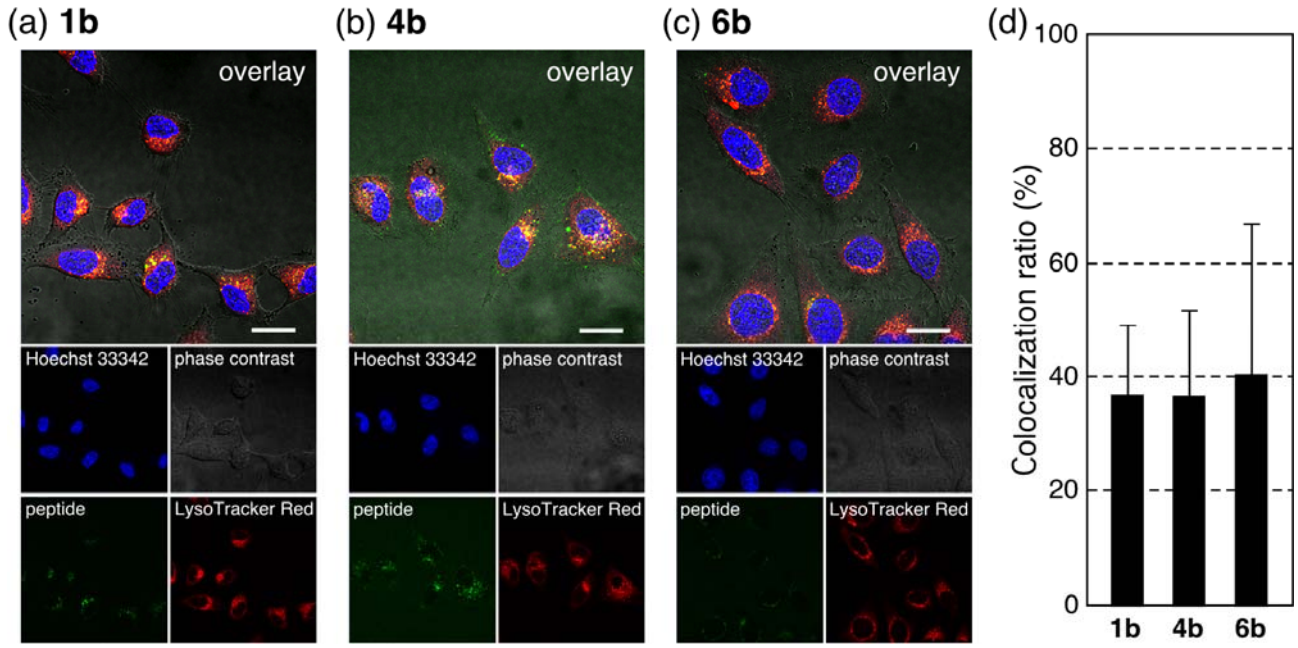

Figure 5. Intracelluar distribution of peptides **1b** (a), **4b** (b), and **6b** (c) (green). Acidic late endosomes/lysosomes and nuclei were stained with LysoTracker Red (red) and Hoechst33342 (blue), respectively. The scale bars represent 20 μm. (d) Quantification of the colocalization of peptides with LysoTracker Red. Error bars represent the standard deviation, n = 15.